Available online at www.sciencedirect.com
ScienceDirect
Bioorganic & Medicinal Chemistry 15 (2007) 1083–1090
Bioorganic & Medicinal Chemistry

Antinociceptive and antiinflammatory activities and QSAR studies on 2-substituted-4,5-diphenyl-1*H*-imidazoles

A. Puratchikody[a] and Mukesh Doble[b,*]

[a]*Department of Pharmaceutical Engineering and Technology, Bharathidasan Institute of Technology, Bharathidasan University, Tiruchirappalli 620024, India*
[b]*Department of Biotechnology, Indian Institute of Technology Madras, Chennai 600036, India*

Received 23 August 2006; revised 6 October 2006; accepted 11 October 2006
Available online 18 October 2006

Abstract—This paper describes the pharmacological evaluation pertaining to antinociceptive (hot plate and tail flick) and antiinflammatory (based on Carrageenan-induced paw oedema) activities, and QSAR studies on 2-substituted-4,5-diphenyl-1*H*-imidazoles. Compounds with phenyl substitution with –F, –Cl, $–NH_2$, $–N(CH_3)_2$, –OH and $–OCH_3$ at the *p*-position showed higher activity than the other substitutions in all the three studies. QSARs developed for the 60 and 120 s hot plate data indicate that the models for both the cases not only fit the data very well ($R^2 > 0.9$, $R^2_{adj} > 0.86$), but also have very good predictive capability ($q^2 > 0.81$). The descriptors used in the model relate to surface area, volume, dipole moment and ADME properties of the molecule. Good QSARs for the 60 and 120 s tail flick data are developed. The models fit the data well ($R^2 > 0.8$, $R^2_{adj} > 0.74$), and in addition have good predictive capability ($q^2 > 0.66$). Surface area, specifically polar surface area, HOMO and molecular connectivity index appear in the models. Very good QSAR model is developed for the antiinflammatory data ($R^2 = 0.86$, $R^2_{adj} = 0.822$ and $q^2 = 0.64$) with aqueous solubility, number of hydrogen bond donor groups, surface area and principal moment of inertia as the molecular descriptors.
© 2006 Elsevier Ltd. All rights reserved.

1. Introduction

Imidazole derivatives have occupied a unique place in the field of medicinal chemistry. They have wide range of biological activities. They are well-known analgesics,[1] antiinflammmatory,[2] antiparasitic,[3] platelet aggregation inhibitors,[4] and antiepileptic agents.[5] Imidazole can be found in many other drugs such as dacarbazine,[6] metronidazole,[7] cimetidine,[8] flumazenil,[9] thyroliberin,[10] methimazole,[11] pilocarpine,[12] and etomidate[13] which are used as antineoplastic, antibiotic, antiulcerative, benzodiazepine antagonist, prohormone, antihyperthyroid, muscarinic receptor antagonist and hypnotic agents, respectively. In view of such reports and in continuation to our work on the imidazole derivatives,[14,15] we report here the in vivo pharmacological evaluation and QSAR studies on new 2-substituted-4,5-diphenyl-1*H*-imidazoles.

Several papers report QSAR studies on benzimidazole derivatives. The in vitro activity of benzimidazole chloroaryloxyalkyl derivatives against *Salmonella typhi* O-901 and *Staphylococcus aureus* A 15091 is found to depend on three molecular descriptors namely, HOMO (Highest occupied molecular orbital) energy, hydration energy and number of primary carbon atoms of the molecule.[16] 2-Aminobenzimidazole moiety connected to the 4 (5) position of an imidazole ring through di- or tri-methylene chains exhibits activity on rat brain membranes and the activity is found to correlate with log *P* through a parabolic relationship.[17] Activities of benzimidazoles against *Bacillus subtilis* also indicate a similar relationship. Sener et al. have developed the QSAR of activity of benzimidazoles against *Klebsiella pneumoniae*[18] and concluded that the more potent compound possesses an oxazolo pyridine ring system substituted with an electron-withdrawing group at position 5 and benzyl moiety at position 2.[19] In addition, they found that the activity of these compounds against *Candida albicans* highly correlated with LUMO (lowest unoccupied occupied molecular orbital), molecular weight, resonance effect and HOMO.[20] Oxazolo pyridine ring system with the substitution of a benzyl moiety at position 2 exhibits good activity against *K.*

Keywords: 2-Substituted-4,5-diphenyl-1*H*-imidazoles; Molecular descriptors; Surface area; HOMO; Genetic function algorithm.
* Corresponding author. Tel.: +91 44 22374107; fax: +91 44 22374102; e-mail: mukeshd@iitm.ac.in

0968-0896/$ - see front matter © 2006 Elsevier Ltd. All rights reserved.
doi:10.1016/j.bmc.2006.10.025

pneumoniae and groups which possessed hydrogen-accepting capability improved the activity.[21]

2. Results and discussion

Compounds listed in Table 1 were obtained by the method outlined in Figure 1. The synthesis of **1**–**25** was carried out by condensation of benzil with ammonium acetate and appropriate aldehyde(s). Substituted benzaldehyde(s) is used to give compounds **1**–**21**. Aldehyde containing alkyl, alkenyl or styryl unit is used to give compounds **22**–**25**. The yields of **1**–**25** fall in the range of 65–82%. Most of them are colourless crystalline solids. The preparation procedure and properties of these imidazole derivatives have been discussed somewhere else in more detail.[14,15]

Table 1 shows the result of antinociceptive and antiinflammatory studies. In the hot plate and tail flick models, there was no significant difference in the mean predrug reaction time among the different groups. Thirty minutes after the administration of the drug, reaction time increased significantly for the test and standard groups when compared to the predrug reaction time. The compounds **12**, **13**, **17**, **18**, **19** and **21** showed their potency as antinociceptive agents by their greater increase in reaction time. The compounds **2**, **4**, **6**, **7**, **10** and **11** increased the pain threshold significantly after 30 min. The groups such as –F, –Cl, $–NH_2$, $–N(CH_3)_2$, –OH and $–OCH_3$ at the *p*-position of the phenyl substituted imidazoles (compounds **12**, **13**, **17**, **18**, **19** and **21**, respectively) produced significant antinociceptive activi-

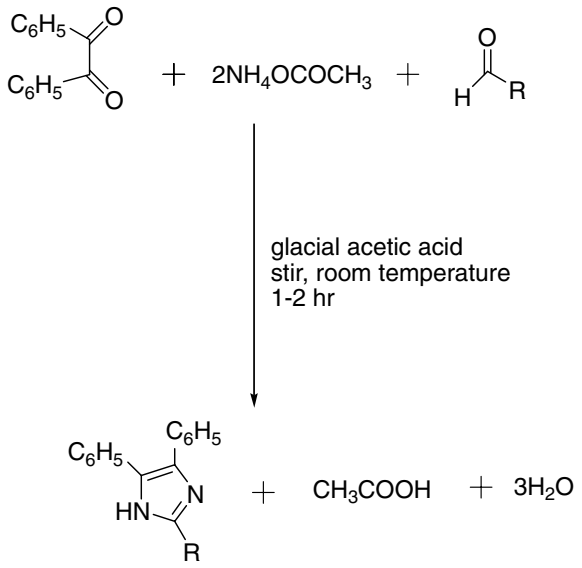

Figure 1. Synthesis scheme.

Table 1. Compounds synthesised and their corresponding biological activity

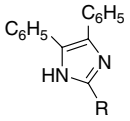

Compound	R	Hot plate method. Experiments performed after (in s)					Tail flick method. Experiments performed after (in s)					% reduction in paw volume
		0	15	30	60	120	0	15	30	60	120	
1	Phenyl	4.63	4.58	5.28	6.07	6.1	4.12	4.13	4.67	5.12	5.78	30.24
2	2-Chlorophenyl	4.67	4.62	6.25	8.2	9.01	4.2	4.14	5.78	7.27	8.85	62.8
3	2-Nitrophenyl	4.5	4.52	4.62	4.67	4.71	4.09	4.1	4.38	4.38	4.39	30.24
4	2-Hydroxyphenyl	4.89	4.93	6.32	8.59	9.16	4.2	4.18	5.82	7.53	9.12	60.47
5	2-Methylphenyl	4.5	4.55	4.67	4.79	5.79	4.11	4.12	4.52	4.98	5.52	18.61
6	2-Methoxyphenyl	4.9	4.94	6.89	8.65	9.25	4.21	4.21	5.98	7.64	9.23	65.12
7	3-Chlorophenyl	4.68	5.14	6.18	7.78	8.91	4.12	4.12	4.98	6.89	8.18	55.82
8	3-Nitrophenyl	4.55	4.56	4.6	4.62	5.62	4.09	4.09	4.36	5.74	5.82	4.66
9	3-Methylphenyl	4.56	4.6	4.63	4.67	5.72	4.1	4.1	4.48	5.89	5.93	9.31
10	3-Methoxyphenyl	4.67	5.02	6.15	7.42	8.79	4.12	4.12	4.56	6.75	7.99	37.21
11	4-Hydroxy-3-methoxyphenyl	4.68	5.23	6.2	7.92	8.99	4.16	4.12	5.57	7.18	8.34	58.14
12	4-Fluorophenyl	4.78	4.93	7.5	9.33	10.83	4.55	4.87	7.14	8.92	10.67	79.07
13	4-Chlorophenyl	4.66	4.9	7.43	8.98	10.35	4.52	4.67	6.92	8.37	10.5	81.4
14	4-Bromophenyl	4.45	4.65	6.37	6.38	6.38	4.2	4.45	5.33	6.5	6.83	74.42
15	4-Iodophenyl	4.45	4.64	5.33	6.18	6.18	4.16	4.26	5.21	5.89	6.5	27.91
16	4-Nitrophenyl	4.37	4.6	4.66	5.82	5. 83	4.13	4.14	5.09	5.12	5.13	25.59
17	4-Aminophenyl	4.48	4.69	7.01	8.25	10.08	4.22	4.27	6.18	7.77	10.05	81.4
18	4-Dimethylaminophenyl	4.5	4.76	7.16	8.33	10.3	4.26	4.45	6.32	7.93	10.18	69.77
19	4-Hydroxyphenyl	4.55	4.81	7.21	8.63	10.33	4.4	4.48	6.79	8.18	10.33	83.73
20	4-Methylphenyl	4.35	4.5	4.62	4.83	4.82	4.14	4.14	4.82	4.82	4.89	11.63
21	4-Methoxyphenyl	4.87	5.02	7.89	9.67	10.87	4.58	4.98	7.45	9.17	10.83	86.05
22	H	4.66	4.83	4.83	5.05	5.2	3.9	3.92	4.01	4.01	4.02	20.94
23	Methyl	4.65	5.1	5.33	5.47	5.52	4.12	4.17	4.28	4.35	4.35	25.59
24	2-Propenyl	4.66	5.08	5.12	5.33	5.47	3.98	4.02	4.23	4.27	4.29	32.56
25	2-Styryl	4.67	5.17	5.58	5.94	6.12	4.16	4.28	0	4.68	4.75	55.82

ty ($P < 0.001$). Presence of groups like –Cl, –OH and –OCH_3 at the *o*-position of the phenyl substituted imidazoles (compounds **2**, **4** and **6**, respectively) showed moderately significant activity ($P < 0.01$). Substitution of groups such as –Cl, –OCH_3 and –4-OH–3-OCH_3 at the *m*-position of the phenyl substituted imidazoles (compounds **7**, **10** and **11**, respectively) exhibited significantly less activity ($P < 0.02$).

In the acute inflammation model, the compounds **12**, **13**, **18** and **19** showed maximum inhibition of carrageenan-induced rat paw oedema at the end of 3 h. Moreover, oedema suppressant effect of the compounds **2**, **4**, **6**, **7**, **11**, **14**, **17**, **21** and **25** was found to be moderately significant as compared to control ($P < 0.01$). Carrageenan-induced hind paw oedema is the standard experimental model of acute inflammation. Carrageenan is the phlogistic agent of choice for testing antiinflammatory drugs as it is not known to be antigenic and is devoid of apparent systemic effects. Moreover, the experimental model exhibits a high degree of reproducibility.[22] Carrageenan-induced oedema is a biphasic response. The first phase is mediated through the release of histamine, serotonin and kinins, whereas the second phase is related to the release of prostaglandin and other slow-reacting substances which peak at 3 h.[23] The compound **21** exhibited maximum inhibition of 86.0% and, **25** showed a minimum inhibition of 55.8%, while the standard drug indomethacin showed an inhibition of 95.3% in the carrageenan-induced rat paw oedema (acute) model. The inhibition of the test drugs was however less than that of the standard drug indomethacin.

Figures 2–4 show the cluster analysis of the activity data for the hot plate, tail flick and antiinflammatory studies, respectively. Compounds **12** (4-fluorophenyl), **13** (4-chlorophenyl), **17** (4-aminophenyl), **18** (4-dimethylamino- phenyl), **19** (4-hydroxyphenyl) and **21** (4-methoxyphenyl) exhibit highest activity in all the three in vivo studies and are located in a single cluster. This is possibly because these compounds have electron-donating groups. In addition compounds having N or O are more hydrophilic than the other groups. Compound **1** (phenyl) exhibits the lowest activity in all the three in vivo studies, probably because of its hydrophobic nature.

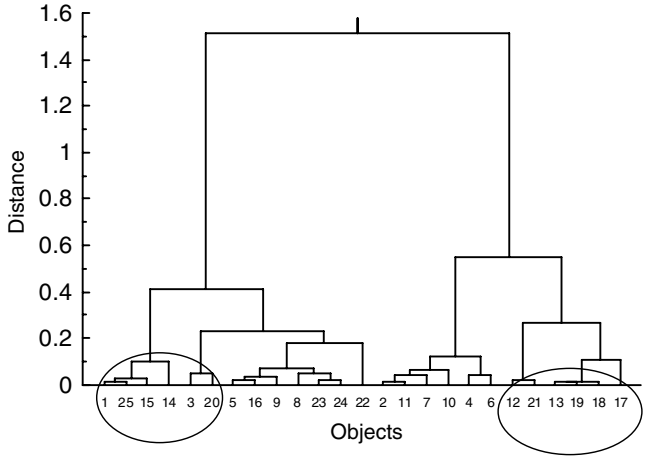

Figure 2. Cluster analysis of hot plate data (120 s data).

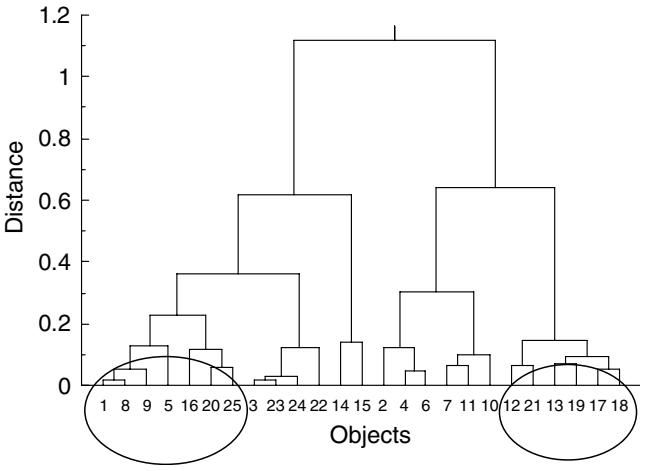

Figure 3. Cluster analysis of tail flick data (120 s data).

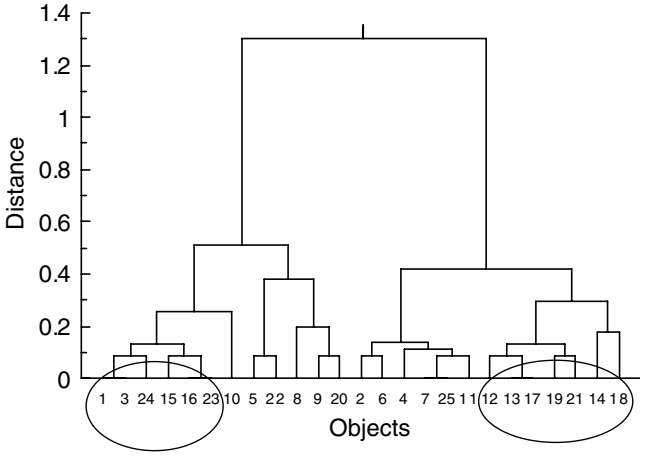

Figure 4. Cluster analysis of antiinflammatory data.

Table 2 shows the results of the ANOVA of the data from hot plate studies. Statistically significant difference is seen between the response time data collected at various time intervals ($F = 23.5$, $P < 0.001$), with a steady increase in the means of 25 data values. The mean of the hot plate response time increases from 4.6 to 7.6 s when the data collection is carried out at 120 instead of 0 s. Table 3 shows the results of the ANOVA of the data from tail flick studies. Statistically significant difference is seen between the response time data collected at various time intervals ($F = 24.38$, $P < 0.001$), with a steady increase in the means of the 25 data values. The mean of the tail-flick response time is 4.2–7.3 s when the data collection is carried out at 0 and 120 s, respectively.

Table 4 lists the best QSAR models for the 60 and 120 s hot plate data. The results indicate that the models developed for both the cases not only fit the data well ($R^2 > 0.9$), but also have very good predictive capability ($q^2 > 0.81$). Description of the descriptors used in the

Table 2. One-way ANOVA of the data from hot plate method

Experiments performed after (s)	0	15	30	60	120
Mean of 25 data (s)	4.61	4.81	5.91	6.86	7.61
Variance	0.022	0.053	1.1518	2.908	4.762
Factor	Sum of squares	Degrees of freedom	Mean SS	F (cal)	
Between groups	166.89	4	41.72	23.445	($^*P \leqslant 0.001$)
Within groups	213.54	120	1.779		
Total	380.43	124			

Table 3. One-way ANOVA of the data from tail flick studies

Experiments performed after (s)	0	15	30	60	120
Mean of 25 data (s)	4.19	4.26	5.37	6.37	7.3
Variance	0.026	0.066	1.03	2.50	5.64
Factor	Sum of squares	Degrees of freedom	Mean SS	F (cal)	
Between groups	181.42	4	45.36	24.38	($^*P \leqslant 0.001$)
Within groups	221.34	119	1.86		
Total	402.77	123			

Table 4. Best QSAR model for the data from hot plate method

	Regression model	R^2	R^2_{adj}	q^2	F	MSSE
Experiments performed after 60 s	Activity = 0.696 + 0.413 * Jurs-TASA − 2.447 * ADME_Absorption-T2-2D − 0.0397 * Jurs-SASA + 6.233 * ADME_BBB_2D − 0.213 * Jurs-PNSA-3 + 0.00514 * Weiner	0.896	0.862	0.806	25.97	0.289
Experiments performed after 120 s	Activity = −10.363 + 0.382 * Jurs-RNCS − 1.776 * ADME_Absorption_T2_2D + 0.0992 * Vm − 0.0955 * ADME_PSA_2D + 0.146 * Dipole-mag	0.922	0.902	0.868	45.1	0.35

Table 5. Details of the descriptors used in the QSAR models listed in Table 4

Descriptors name	Explanation
Jurs-TASA	Total hydrophobic surface area: sum of solvent-accessible surface areas of atoms with absolute value of partial charges less than 0.2.
Jurs-SASA	Total molecular solvent-accessible surface area.
Jurs-PNSA-3	Atomic charge weighted negative surface area: sum of the product of solvent-accessible surface area X partial charge for all negatively charged atoms.
Vm	Molecular volume inside the contact surface. Molecular volume is related to binding and transport.
Wiener	The sum of the chemical bonds existing between all pairs of heavy atoms in the molecule.
Dipole-mag	Indicates the strength and orientation behaviour of a molecule in an electrostatic field.
ADME_BBB_2D	Blood brain barrier permeation-depends on H-bonding capacity, local hydrophobicity, molecular size, lipophilicity and flexibility.
ADME_PSA_2D	ADME polar surface area.
ADME_Absorption_T2_2D	Multivariate distance among nitrogen, oxygen atoms and attached hydrogen atoms from van Der Waals polar surface area.

models is listed in Table 5. All the descriptors relate to surface area, volume, dipole moment and ADME (Absorption, Distribution, Metabolism and Excretion) properties of the molecule. Dipole moment is caused due to the asymmetry in the 3-D structure of the molecule. Molecular volume, shape and hydrophobicity of the substituent group are found to affect fungicidal activity of benzimidazoles.[24] Figure 5 compares the hot plate data and model predictions in the form of a parity plot for the experiments carried out at 120 s.

Table 6 lists the best QSAR models for the 60 and 120 s tail flick data. The results indicate that the models developed for both the cases not only fit the data well ($R^2 > 0.8$), but also have good predictive capability ($q^2 > 0.66$). In addition to surface area, specifically polar

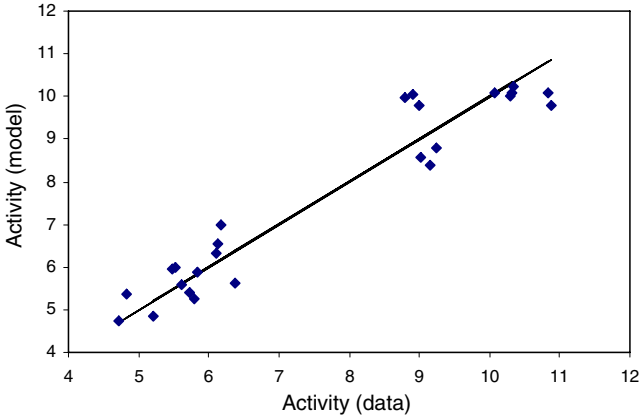

Figure 5. Parity plot of hot plate data (experiments carried out at 120 s).

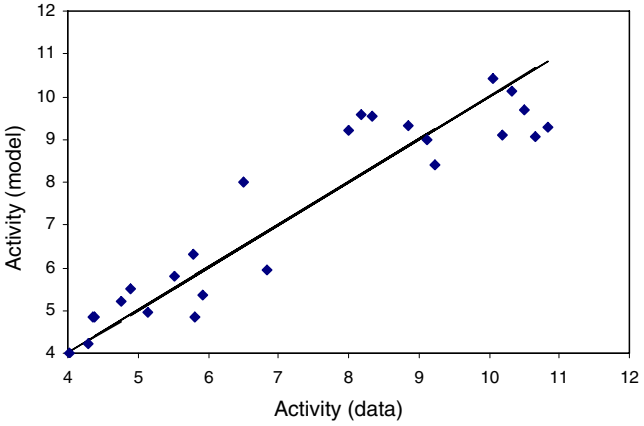

Figure 6. Parity plot of tail flick data (experiments carried out at 120 s).

surface area, HOMO, the electronic descriptor and molecular connectivity index also appear in the model (see Table 7). HOMO has been identified as a molecular descriptor by others to describe in vitro activity of benzimidazole chloroaryloxyalkyl derivatives against *S. typhi* O-901 and *S. aureus* A 15091.[16,20] The polar surface area is an indication of the hydrophilic nature of the molecule. Relative lyphophilic character, as defined by octanol/water partition coefficient (namely log *P*), is a very important property that determines the biological activity of substituted imidazoles.[25] Figure 6 shows the parity plot of the tail flick experiments carried out at 120 s and the model predictions.

Table 8 lists the best QSAR model for the antiinflammatory data. The model fits the data very well ($R^2 = 0.86$) and also has a good predictive capability ($q^2 = 0.64$). A description of the descriptors used in the models is listed in Table 9. Aqueous solubility, number of hydrogen bond donor groups, surface area and principal moment of inertia are the descriptors that appear in the model for the activity data. Aqueous solubility is an indication of the hydrophilic nature of the molecule. Descriptor that characterises the hydrogen bond donor/acceptor capability is found to be essential to describe the antibacterial activity of substituted benzimidazoles against *K. pneumoniae*.[21] Similar descriptors have been identified by other researchers as well for different imidazoles.[20] Figure 7 compares the antiinflammatory data and model predictions.

3. Conclusions

Imidazole derivatives have a wide-ranging biological activity. In this paper, the determination of antinociceptive and antiinflammatory activities of 2-substituted-4,5-diphenyl-1*H*-imidazoles is reported. The antinociceptive activity is based on hot plate and tail flick methods and the antiinflammatory studies are based on carageenan-induced paw oedema. Compounds with phenyl substitution with –F, –Cl, $–NH_2$, $–N(CH_3)_2$, –OH and $–OCH_3$ at *p*-position showed higher activity than all other substitutions in all the three studies. Electron-donating groups

Table 6. Best QSAR model for data from tail flick method

	Regression model	R^2	R^2_{adj}	q^2	F	MSSE
Experiments performed after 60 s	Activity = −12.254 − 1.9950 * ADME_Absorption_level_2D + 0.3704 * Jurs-RNCS + 15.224 * Jurs-FPSA-1 + 2.4993 * CHI-V-3_P + 0.2030 * HOMO	0.80	0.742	0.665	14.85	0.489
Experiments performed after 120 s	Activity = −10.002 + 3.242 * ADME_BBB_2D − 1.9495 * ADME_Absorption_T2_2D + 0.4206 * Jurs-RNCS + 5.7414 * CHI-V-3_P	0.863	0.836	0.789	31.5	0.74

Table 7. Details of the descriptors used in the QSAR models listed in Table 6

Descriptors name	Explanation
ADME_Absorption_level_2D	The Absorption level is calculated based on the position of each molecule in the polar surface area versus AlogP98 plot.
HOMO	Highest energy level in the molecule that contains electrons molecules with high HOMOs are more able to donate their electrons and are hence relatively reactivity of the molecule.
CHI-V-3_P	Molecular connectivity index.
Jurs-RNCS	Relative negative charge surface area: solvent-accessible surface area of most negative atom divided by descriptor.
Jurs-FPSA-1	Fractional charged partial surface areas.

Table 8. Best QSAR model for data from antiinflammatory study (% reduction in paw volume)

Regression model	R^2	R^2_{adj}	q^2	F	MSSE
Activity = 264.84 + 57.73 * ADME_Solubility − 177.54 * Jurs-RPSA − 9.87 * Jurs-WNSA-3 + 31.43 * Hbond donor + 0.03 * PMI-mag	0.859	0.822	0.642	231.8	93.88

Table 9. Details of the descriptors used in the QSAR model listed in Table 8

Descriptors name	Explanation
ADME_Solubility	Prediction of aqueous solubility.
Jurs-RPSA	Total polar surface area divided by the total molecular solvent-accessible surface area.
Jurs-WNSA-3	Surface-weighted charged partial surface area.
Hbond donor	Number of hydrogen bond donor groups.
PMI-mag	Principal moment of inertia calculated about the principal axes of a molecule.

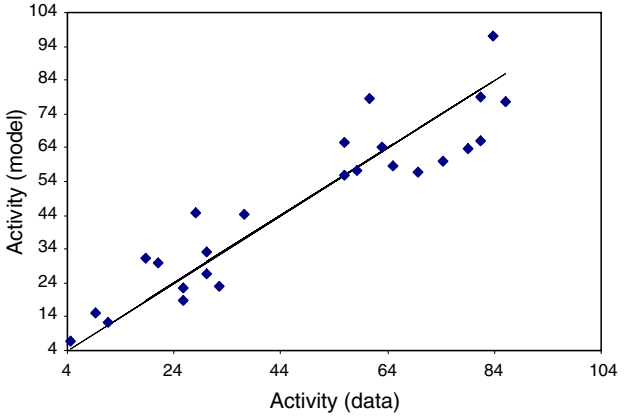

Figure 7. Parity plot of antiinflammatory data (% reduction in paw volume).

and hydrophilicity play an important role in the biological activity. Lowering of activity was observed with hydrophobic groups. Quantitative structure–activity relationships are developed correlating the observed biological activity with structural descriptors. For all the cases the models developed are able to fit the data very well ($R^2 > 0.8$, $R^2_{adj} > 0.74$) with good predictive capability ($q^2 > 0.64$). The molecular descriptors used in the models relate to surface area, volume, dipole moment, ADME, HOMO, molecular connectivity index, aqueous solubility, number of hydrogen bond donor group, and principal moment of inertia. A genetic function algorithm technique is used to select the descriptors from a large pool of calculated molecular properties. This technique is useful in identifying the best descriptors when their number is much larger when compared to the experimental data.

4. Experimental

4.1. Acute toxicity study

Albino mice of both sexes were divided into 125 groups. Each group had 10 animals. They were treated with test drugs (ip) with the dose range from 40 to 220 mg/kg. The animals were observed for mortality until 72 h and the LD_{50} was calculated using graphical method.[26]

4.2. Pharmacology

The test compounds were evaluated for antinociceptive and antiinflammatory activities. Student's t test[27] was performed for all the activities to ascertain the significance of the exhibited activities. The test compounds and the standard drugs were administered in the form of suspension (0.2% Tween suspension as vehicle) in the same route of administration.

4.3. Animal experimentation

Biological evaluation of **1**–**25** was carried out in the Department of Animal Biotechnology, Bharathidasan University, Tiruchirappalli. Animal facility of this institute is approved by CPCSEA (Reg.No.418/a/01/CPCSEA). The experimental protocols for the antinociceptive and antiinflammatory activities have been approved by the Institutional Animal Ethics Committee and conducted according to the guidelines of Indian National Science Academy for the use and care of experimental animals. The animals were maintained at a well-ventilated, temperature-controlled (30 ± 1 °C) animal room for 7 days prior to the experimental period and provided with food and water ad libitum. The animals were acclimatized to laboratory conditions before the test.

4.4. Antinociceptive activity

Hot plate and tail flick methods[28,29] were employed to determine antinociceptive activity. The hot-plate test was assessed on eleven groups of six mice. The Swiss albino mice (20–25 g) were used in the test. One group served as standard (received pentazocine 10 mg/kg ip), the other group served as control (received 0.2% Tween suspension 5 ml/kg, ip). The remaining 25 groups received between 9.5 and 12.58 mg/kg of the compounds **1**–**25** ip. The basal reaction time of the animal was noted by placing the animals in the hot plate at 55 ± 0.5 °C before and 15, 30, 60, and 120 min after the administration of test drugs. Cut-off time was kept at 15 s in order to avoid injury to the tail. Tail flick to radiant heat (Tail-flick apparatus type 812, Hugo Sachs Elektronik, Germany) was used to measure acute nociceptive responses in mice. The Swiss albino mice (20–25 g) were used in this study and worked up as mentioned in the above method. The inten-

sity of the thermal stimulus was adjusted to produce 3–4 s latency in tail-flick response. The latency was measured just before, 15, 30, 60 and 120 min after injections. The trial was automatically terminated at 12 s if a response did not occur (cut-off time). The prolongation of the latency times compared with the values of the control was used for statistical comparison.

4.5. Antiinflammatory activity

Antiinflammatory activity was determined by carrageenan-induced rat paw oedema method.[30] Wistar rats of either sex (120–150 g) were used in this study and worked up as mentioned in the above method. The standard drug used here was indomethacin (10 mg/kg ip). The control group received 0.2% Tween suspension 5 ml/kg ip. All the remaining 25 groups received between 9.5 and 12.58 mg/kg of the compounds **1**–**25** ip. After an hour of test drug administration the animals were injected with 0.05 ml suspension of carrageenan (1.0% w/v in 0.9% NaCl) in the left hind paw planter aponeurosis. The volume of paw was measured using the mercury displacement technique with the help of a plethysmometer (UGO-Basile, Italy). It was measured both in control as well as in standard animals including the test animals at an interval of 1, 2 and 3 h after carrageenan injection. The initial volume of paw was measured immediately before the injection. The increase in paw volume after 3 h was calculated. The percentage inhibition of inflammation after 3 h was calculated by using Eq. 1.

$$\text{Percentage inhibition} = 100[1 - (V_t)/(V_c)] \quad (1)$$

where V_t = Mean relative changes in the paw volume of each of the rats after the administration of carrageenan and test or standard compound.

V_c = Mean relative changes in the paw volume of each of the rats after the administration of carrageenan injection in the control group.

4.6. Modelling methodology

ANOVA, cluster analysis and principal component analysis were performed using a standard statistical software package, Kyplot®. The structure of the various molecules as given in Table 1 was drawn and the energy was minimized by using Universal force field available in Cerius[2] software® (Acceryls Inc, USA). Two hundred and twenty-nine descriptors that include topological, charge, geometrical, aromaticity indices, constitutive properties, quantum mechanics and thermodynamics were evaluated for all the molecules. Several literature reports give a very detailed description of these descriptors.[31–33] A genetic function algorithm (GFA) technique was used to select the descriptors from this large pool for using in the QSAR model.

The GFA uses a genetic algorithm to perform a search over the space of possible QSAR models using the lack of fit (LOF) score to estimate the fitness of each model. Such evolution of a population of randomly constructed models leads to the discovery of highly predictive QSAR. The populations of the models are created by evolving random initial models using a genetic algorithm. GFA can build models using not only linear polynomials but also higher-order polynomials, splines and other nonlinear functions. The goodness of the regression fits were estimated using statistical parameters such as, R^2 (=1 − SSE/TSS), $R^2_{adj}(= 1 - (n-1)(1-R^2)/(n-p-1))$, q^2 (=1 − PRESS/TSS) and F ratio $(=(n-2)R^2/(1-R^2))$ and MSSE (=mean sum of square of error = SSE/n), where TSS = total sum of squares and SSE = sum of squares, PRESS = predictive sum of squares based on leave-one-out method. R^2 and R^2_{adj} are indication of the model fit, while q^2 is an indication of the predictive capability of the model. A large F indicates that the model fit is not a chance occurrence. R^2, R^2_{adj} and q^2 above a value of 0.6 indicate good model fit.

References and notes

1. Ucucu, D.; Karaburn, N. G.; Isikdag, I. *Farmaco* **2001**, *56*, 285.
2. Maeda, S.; Suzuki, M.; Iwasaki, T.; Matsumoto, K.; Iwasawa, Y. *Chem. Pharm. Bull.* **1984**, *32*, 2536.
3. Quattara, L.; Debaert, M.; Cavier, R. *Farmaco (Sci.)* **1987**, *42*, 449.
4. Seko, N.; Yoshino, K.; Yokota, K.; Tsukamoto, G. *Chem. Pharm. Bull.* **1991**, *39*, 651.
5. Puratchikody, A.; Yasodha, A.; Ruckmani, K.; Sarkunam, K.; Nallu, M. *Indian J. Heterocycl. Chem.* **2003**, *14*, 79.
6. Shealy, Y. F.; Krauth, C. A.; Montgomery, J. A. *J. Org. Chem.* **1962**, *27*, 2150.
7. Brogden, R. N.; Heel, R. C.; Speigt, T. M. *Drugs* **1978**, *16*, 387.
8. Brimblecombe, R. W.; Duncan, W. A. M.; Durant, G. J.; Emmet, C.; Gamellin, C. R.; Parsons, M. E. *J. Int. Med. Res.* **1975**, *3*, 86.
9. Hunkeler, W.; Mohler, H.; Pieri, L.; Polc, P.; Bonetti, E. P.; Cumin, R.; Schaffner, R.; Haefely, W. *Nature* **1981**, *290*, 514.
10. Fluoret, G. *J. Med. Chem.* **1970**, *13*, 843.
11. Cooper, D. S. N. *Engl. J. Med.* **1984**, *311*, 1353.
12. Mayorga, A. J.; Cousins, M. S.; Trevitt, J. T.; Coulan, A.; Gianutsos, G.; Salamone, J. D. *Eur. J. Pharmacol.* **1999**, *364*, 7.
13. Godefroi, E. F.; Janssen, P. A. J.; Van der Eycken, C. A. M.; Van Heertum, A. H. M. T.; Niemegeers, C. J. E. *J. Med. Chem.* **1965**, *8*, 220.
14. Puratchikody, A.; Gopalakrishnan, S.; Nallu, M. *Indian J. Heterocycl. Chem.* **2004**, *14*, 149.
15. Puratchikody, A.; Gopalakrishnan, S.; Nallu, M. *Indian J. Pharm. Sci.* **2005**, *67*, 47.
16. Khalafi-Nezhad, A.; Soltani Rad, M. N.; Mohabatkar, H.; Asrari, Z.; Hemmateeneja, B. *Bioorg. Med. Chem.* **2005**, *13*, 1931.
17. Mor, M.; Bordi, F.; Silva, C.; Rivara, S.; Zuliani, V.; Vacondio, F.; Rivara, M.; Barocelli, E.; Bertoni, S.; Ballabeni, V.; Magnanini, F.; Impicciatore, M.; Plazzi, P. V. *Bioorg. Med. Chem.* **2004**, *12*, 663.
18. Yalcin, I.; Aki-Sener, E. *Int. J. Pharm.* **1993**, *98*, l.
19. Sener, E.; Yalcin, I.; Sungur, E. *Quant. Struct-Act. Relat.* **1991**, *10*, 223.
20. Turker, L.; Sener, E.; Yalcin, I.; Akbulut, U.; Kayalidere, I. *Sci. Pharm.* **1990**, *58*, 107.
21. Yalcin, I.; Sener, E. *Int. J. Pharm.* **1993**, *98*, 1.
22. Winter, C. A.; Risley, E. A.; Nuss, G. W. *Proc. Soc. Exp. Biol. Med.* **1962**, *111*, 544.

23. Vinegar, R.; Schreiber, W.; Hugo, R. *J. Pharmacol. Exp. Ther.* **1969**, *166*, 96.
24. Takahashi, J.; Kirino, O.; Takayama, C.; Nakamura, S.; Noguchi, H.; kato, T.; Kamoshita, K. *Pestic. Biochem. Phys.* **1988**, *30*, 262.
25. Ertepinar, H.; Gok, Y.; Geban, O.; Ozden, S. *Eur. J. Med. Chem.* **1995**, *30*, 171.
26. Miller, L. C.; Tainter, M. L. *Pro. Soc. Exp. Biol. Med.* **1994**, *57*, 261.
27. Armitage, P. *Statistical Methods in Medical Research*, 1st ed.; Blackwell Scientific Publications: London, 1971, pp 217.
28. Hosseinzadeh, H.; Ramezani, M.; Salmani, G.-A. *J. Ethnopharmacol.* **2000**, *73*, 379.
29. D'Amour, F. G.; Smith, D. L. A. *J. Pharmacol. Exp. Ther.* **1941**, *72*, 74.
30. Vetrichelvan, T.; Jegadeesan, M. *Indian J. Pharmacol.* **2003**, *35*, 388.
31. Todeschini, R.; Lasagni, M.; Marengo, E. *J. Chemomet.* **1994**, *8*, 263.
32. Todeschini, R.; Consonni, V. *Handbook of Molecular Descriptors*; Wiley-VCH: Weinheim, 2000.
33. Karelson, M. *Molecular Descriptors in QSAR/QSPR*; Wiley Interscience: NewYork, 2000.